Measurements of Solid Concentration in a Downward Vertical Gas–Solid Flow

T. Schiewe, K. E. Wirth, and O. Molerus
Institut für Verfahrenstechnik, University of Erlangen-Nürnberg, 91058 Erlangen, Germany

K. Tuzla, A. K. Sharma, and J. C. Chen
Dept. of Chemical Engineering, Lehigh University, Bethlehem, PA 18015

New results from experiments performed in a 15-cm-diameter downflow fast-fluidized bed are presented. Tests were conducted at room temperature and near atmospheric pressure, with 125-μm glass beads. Superficial gas velocities range from 0 to 6.6 m/s. Two different measurement techniques — gamma-absorption tomography and capacitance sensing — were applied to the gas–solids flow in the downer tube. The average local solid fractions from both measurement techniques are compared for various operating conditions of the gas–solid flow. In general, good agreement was obtained between the solid concentration measurements from both measurement techniques. It is demonstrated that combined use of both measurement techniques offers the best chance to get time-average information about the concentration distribution over the whole cross section.

Introduction

For numerous heterogeneous catalytic reactions the conversion of the feeds to the desired product is accompanied by consecutive and/or side reactions, which lead to a decrease in selectivity and yield. These kinds of reactions require a gas–solid reactor with a narrow residence-time distribution for the gas and solid phase to obtain good reaction control. In the literature a novel type of reactor, the so-called downer, with gas and solid particles moving in the direction of gravity, is proposed for that purpose (Zhu et al., 1995; Wang et al., 1996).

The characterization of the gas–solids flow inside this reactor, including the knowledge about the solids distribution in the tube cross section, is the basis for modeling the gas–solids flow and optimization of the reactor.

Several measurement techniques are used to study the local solids concentration in vertical gas–solid flows with the main flow direction against gravity—the so-called circulating fluidized beds or riser reactors. A survey of these techniques is given by Louge (1997). Among these, the capacitance method and gamma-absorption tomography are suitable for measurement of a wide range of local solid concentrations, from dense bed to pneumatic transport conditions. Herb et al. (1989) used the capacitance method to measure local solid concentrations in the riser of a circulating fluidized bed. Similarly, gamma-absorption tomography was used by Seville et al. (1986) and Galtier et al. (1989) to determine solid concentrations in riser beds. Although both of these methods are applicable to downer flows, to date there has been only limited data available for downers (Zhu et al., 1995) and these give only pressure-drop measurements.

In this study, two different measurement techniques—gamma-absorption tomography and capacitance sensing—have been applied to the gas–solids flow in a downer tube. A comparison of the results from both experimental methods provides data on solid concentration distribution in the downer, and points out the advantages and disadvantages of both techniques.

Experimental

Downer setup

The downer setup is shown in Figure 1. The downer (4) consists of tube elements made of stainless steel. Between the stainless-steel elements there are three 0.25-m-long glass

Correspondence concerning this article should be addressed to K. Tuzla.

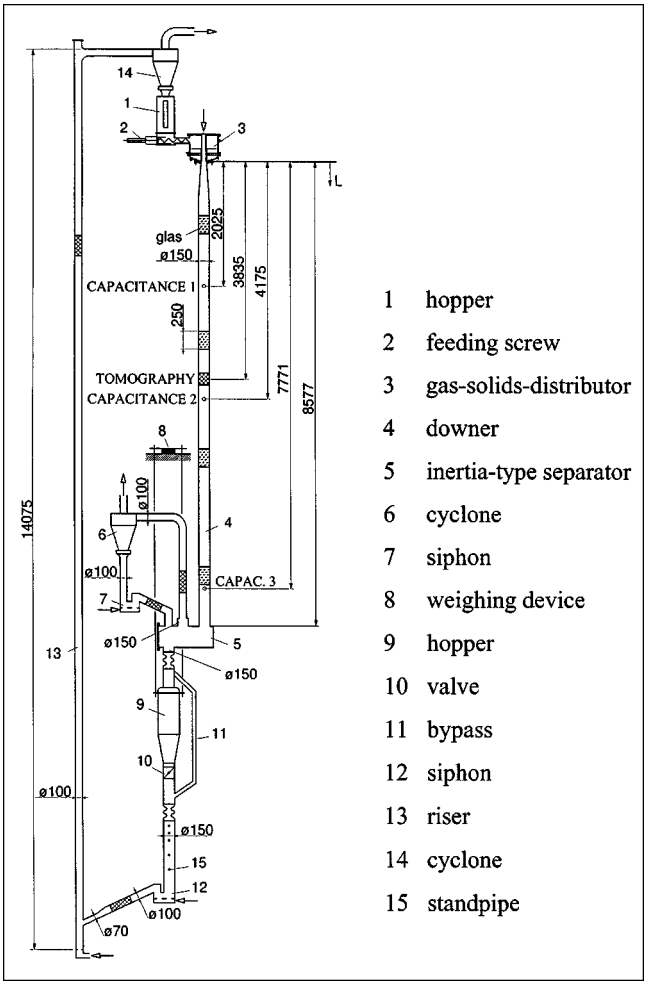

Figure 1. Downer loop.

tube elements for visualization of the flow. The inner diameter of the tube is 0.15 m, and the total downer length is 8.6 m. The solids are fed into the downer at the top with the help of a screw feeder (2) and a special gas–solids distributor (3). Details of this device can be found elsewhere (Schiewe, 1997). At the bottom of the downer, the solids are separated from the gas in two stages (5–7). The first stage consists of an inertial separator, while the second stage is a cyclone separator. The solids are collected in a hopper (9) and then sent into a standpipe (15) for recirculation through a riser (13), another cyclone separator (14), and a hopper (1).

Gas flow rate through the downer is measured by orifice meters. There are 21 differential pressure transducers along the length of the downer to measure axial pressure profile with respect to the pressure at the top of the downer. The solid flux circulating through the downer was measured with the help of a quick-closing valve (10) and by weighing the variation in solid accumulation in the hopper (9) above the valve. Experiments were carried out with glass beads (d_p = 125 μm; ρ_s = 2480 kg/m^3) and air at ambient conditions. Superficial gas velocities have been varied in the range of 0 to 6.6 m/s, and solids mass fluxes ranged up to 100 kg/(m^{2}s).

Gamma-absorption tomography

In order to measure the solids distribution in the cross section of the downer, one of the techniques used is gamma-absorption tomography. The tomography system is located midway along the downer tube, 4.18 m below the gas–solid distributor, as indicated in Figure 1. The setup of the measuring device is shown in Figure 2. From a Cs^{137} source, a narrow gamma-ray beam (average width in the tube cross section was 4 mm) is emitted. After crossing the downer, the impulse rate intensity of the beam is measured with a NaJ-scintillation detector. Using the measured intensities with and without a gas–solids flow, I and I_0, respectively, the average solids concentration $\overline{\epsilon_s}$ along the path of the gamma-ray beam S can be calculated using Lambert–Beer's law:

$$\overline{\epsilon_s} = \frac{1}{\eta_s \cdot \rho_s \cdot S} \cdot \ln \frac{I_0}{I}, \qquad (1)$$

where η_s is the mass absorption coefficient of the solids. The absorption due to the gas can be neglected in comparison to the solids. By moving the gamma-ray source and the detector stepwise over the entire cross section of the downer, a series of line-averaged solids concentrations giving the so-called projection of the pipe cross section can be measured. The exact positioning of the device is controlled by incremental encoders. Two source-detector pairs with rectangular orientation to each other were used. They were moved parallel by stepping motors, mounted on a rotatable platform. This allows us to get two projections of the solids distribution simultaneously at each orientation of the platform. Another pair of projections have been obtained by turning the platform by 45 degrees. Test runs show that a total of four projections are needed to achieve sufficient accuracy of the reconstruction if an algebraic reconstruction technique (ART) is used to reconstruct the solids distribution, (Schiewe, 1997). Due to limited intensity difference of radioactive decay, a minimum recording time at each position is necessary to achieve a given concentration resolution. As a consequence, this technique only offers the chance of getting time-averaged solids concentrations. Nearly one-third of the total measurement time for

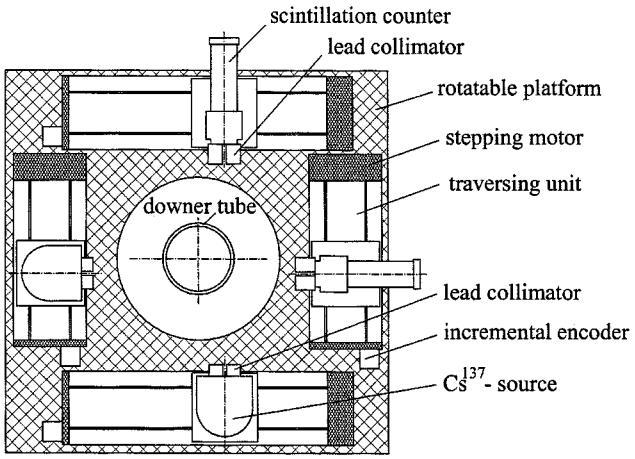

Figure 2. Gamma-absorption tomography system.

one projection is needed to get the projection value on the edge of the tube wall, because at this location the path length S inside the tube approaches zero, and one needs time to make sure that I and I_0 are statistically independent of each other.

In order to keep the total measurement time for each projection to a minimum, the recording of the intensities at these positions has been left out. Theoretical simulations show that even with this omission, the reconstruction of the solids distribution is accurate, except for some pixels directly at the tube wall (Schiewe, 1997). The gamma-ray sources and the detectors used are commercially available. The space resolution of the gamma-ray tomograph is a pixel with a side length of 4 mm. The main advantages of this technique are the nonintrusive measurement of the line-averaged solids concentration, the insensitiveness to electrostatic charging of the gas–solids flow in the downer, and the comparatively small cost to get the solids distribution of the gas–solids flow in the whole cross section. The mass absorption coefficient, η_s, in Eq. 1 depends on the composition of the solid material and the energy of the radiation generated by the source. This constant coefficient can be determined from tables or by one experiment. The method needs no additional calibration. After this one time calibration, the concentration can be determined from measured intensity. Beyond this, the robust setup can also be carried and used at an industrial site as a further benefit. The main restriction of this technique is the exclusive recording of the time-averaged values of the solids concentration due to limited difference on intensity of radioactive decay.

Measurements with capacitance probes

Local-transient solids concentrations were measured using a needle capacitance probe, as illustrated in Figure 3. The probe consisted of an external sheath of 2.4 mm diameter that served as the ground electrode. A central needle 0.5 mm in diameter extended from the end of the sheath for a length of 6 mm, serving as the potential electrode. Within the sheath, a concentric metal tube, electrically insulated from both the outer sheath and the central needle, serves as an active guard to reduce parasitic capacitance. The effective sensing volume of this probe is the cone-shaped region around the exposed length of the central needle; this region was approximately 2.4 mm at the base and 6 mm high. This dimension was selected with the assumption that the measurement volume is smaller than the typical cluster size but orders of magnitude larger than individual particle size. This assumption was based on prior experience with upward fast fluidization. Additional details of this capacitance probe and its circuitry are given in Soong (1992) and Herb (1990). The probe was bench calibrated using mixtures of glass beads in petroleum jelly with known volume concentrations. This technique has been successfully utilized by previous investigators Herb et al. (1989) and Soong et al. (1995). These bench calibration results showed reasonable agreement with the theoretical Maxwell relationship between the solids concentration and the effective dielectric constant of the two-phase mixture (see Soong et al., 1993). An additional calibration step is usually necessary to account for the leakage capacitance resulting from charged gas-particles. This calibration is usually made by comparing the measurements to cross-sectionally averaged solid concentrations obtained from pressure-drop gradients, or from gamma tomography, to the measured concentrations with the capacitance probe. In the present work, particle concentrations are presented in a nondimensional form, which eliminated any additional calibration procedure due to charged particles. This normalization procedure is discussed later (see Eq. 2).

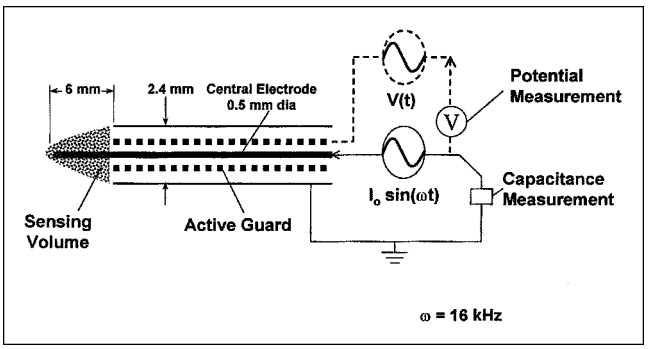

Figure 3. Capacitance probe.

Results and Discussion

Axial pressure profiles

Integral information about the axial development of the gas–solids flow can be obtained by pressure-profile readings. Figure 4 shows the axial increase of pressure, in reference to the first pressure tap at the beginning of the downer tube, for a specific solids mass flow rate of $\dot{m}_S \approx 50$ kg/(m^{2}s) and three different superficial gas velocities. For the limiting case of zero gas velocity, where the particles move down the tube only by the force of gravity, a constant pressure gradient is observed along nearly the entire tube length. This indicates that a fully developed flow is reached after a short development zone of about 0.5 m. Increasing the gas velocity increases the length of the development zone, as indicated by a delayed approach to zone of constant pressure gradient. This increase is accompanied by higher pressures at the beginning of the tube, which are caused by a deceleration in the gas–solids flow inside the diffuser, which provides a transition from the distributing device to the cylindrical part of the

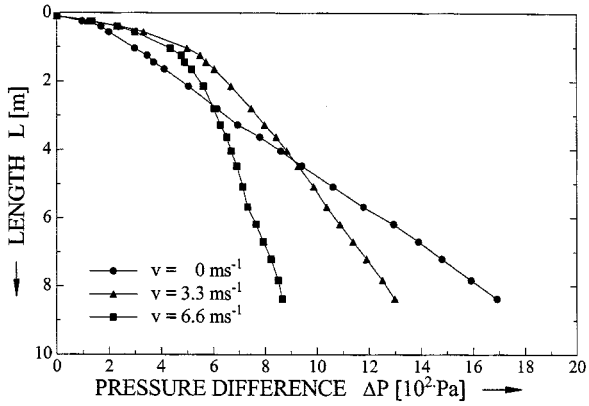

Figure 4. Measured pressure profiles for different superficial gas velocities: $G_s \approx 50$ kg/(m^2·s).

downer tube. With increasing gas velocity, the length of this development zone increases, reaching a length of approximately 3 m for the case of v = 6.6 m/s. It should be noted from the profiles that the tomography setup located at L = 3.84 m is in the zone of fully developed flow for the conditions of the present tests.

Gamma-absorption tomography

All of the gamma-absorption tomography results reported in this article are from the middle of the downer tube, 3.84 m below the gas–solid distributor. Furthermore, reported experimental concentrations measured by the gamma-absorption tomography are time-average results for about a 2-h operation. Typical results obtained from tomography for different operating conditions of the downer are shown in Figure 5. The plots illustrate the solids distribution for a solids mass flux of approximately 50 kg/(m^{2}s) with different superficial gas velocities. For each plot a different solids concentration scale is used to get the best resolution.

If the particles move down the tube only by the force of gravity—without a superimposed gas-flow (v = 0 m/s)—the solids distribution is observed to be in the shape of a parabola, with the maximum concentration at the tube wall and the minimum concentration in the middle of the tube (Figure 5a). With a gas flow corresponding to a superficial gas velocity of 3.3 m/s, particle distribution in the cross section becomes more even (Figure 5b). Increasing the gas velocity further, to a value of v = 6.6 m/s, the solid particles start to segregate and form strands of solids. A sample of a solid strand formation is observed in Figure 5c, which shows solids concentrated in the right quadrant of the downer, with few particles in the remaining area of the cross section (Figure 5c). These solid concentrations, measured by gamma tomography, were compared to the solid concentrations calculated from pressure-drop measurements. In order to do this, the local con-

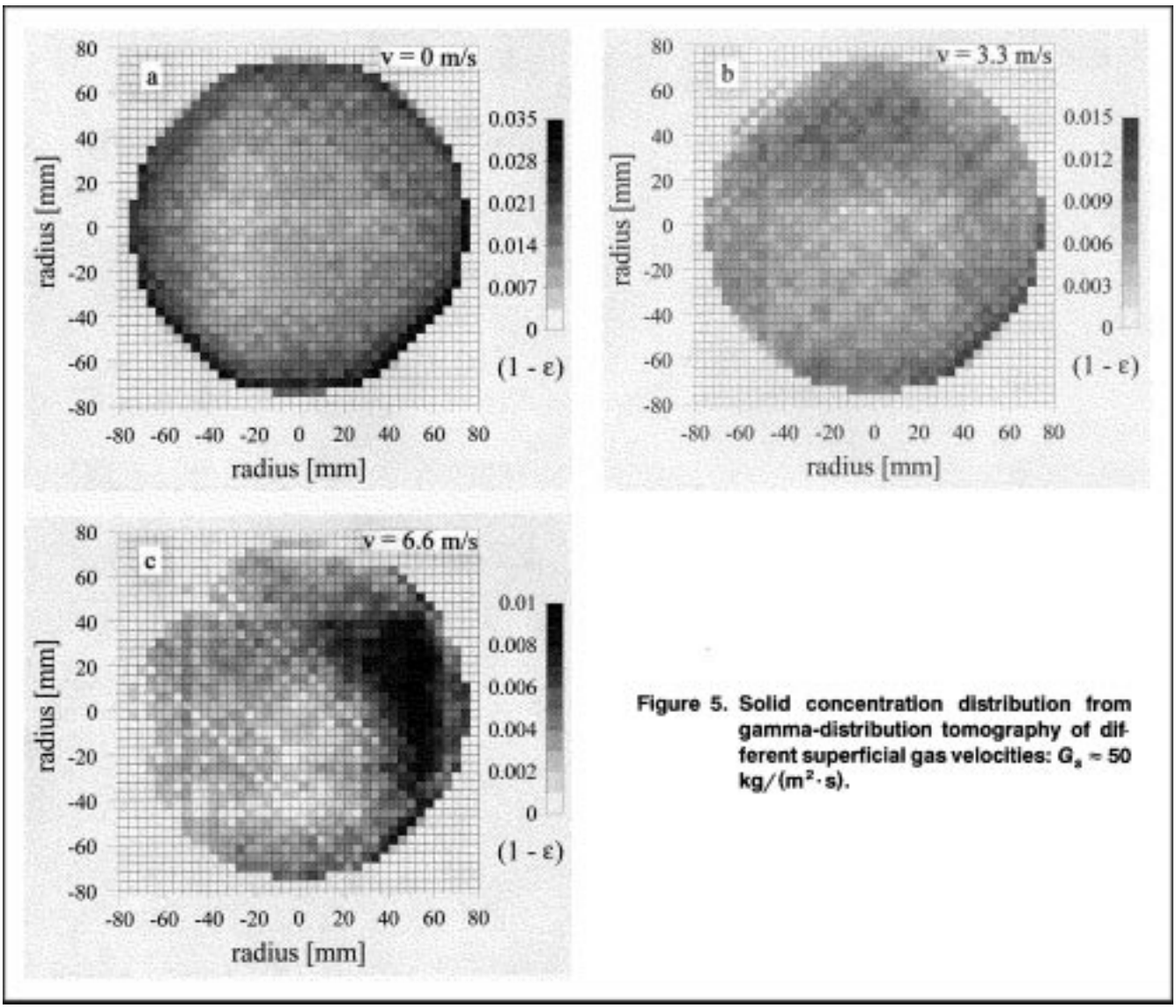

Figure 5. Solid concentration distribution from gamma-distribution tomography of different superficial gas velocities: G_s = 50 kg/(m^2·s).

centrations measured by gamma absorption tomography were integrated to calculate cross-sectionally averaged solids concentrations, $\langle\overline{\epsilon_s}\rangle$. The agreement of these cross-sectionally averaged values was good. The difference between the two cross-sectionally averaged solids concentrations was within ± 5% of the measured value.

The objective of this article is the comparison of two different measurement techniques. It is therefore beyond the scope here to give an explanation for the different flow patterns that depend on the working conditions of the downer setup. Details concerning that subject may be found in Schiewe (1997). In the context of this article, the different flow patterns are used to illustrate the effectiveness and the correspondence of the measurement techniques.

Capacitance probe readings

The capacitance probe readings reported here were recorded from three different locations on the downer. These elevations, 1, 2, and 3, are 2.03, 4.18, and 7.77 m from the gas–solid distributor. At each elevation, the sensing tip of the probe was placed at various radial locations in the downer by inserting it through the side of the downer tube. The radial locations referred to in this article represent the location of the base of the probe sensing tip in reference to the center line of the downer tube.

A typical time trace of transient solid concentration ϵ_s is shown in Figure 6, for downward fluidization, with v_g of 1 m/s and G_s of 89 kg/m^2/s. This sample trace was obtained with the sensing probe located 4.18 m below the feed point, at a radial position close to the downer wall, that is, with the base of the probe sensing tip flush with the inside surface of the downer wall. The oscillatory driving frequency for the capacitance circuit was 16 kHz, and measurements were recorded with a sampling frequency of 5 kHz. The data shown in Figure 6 represent observations over a 9-s-time span, with clearly discernible oscillations in the local instantaneous solid concentrations. Also indicated on this figure is the time-averaged solids concentration, $\overline{\epsilon_s}$, with a value of 0.0175, at this local position for this particular operating condition.

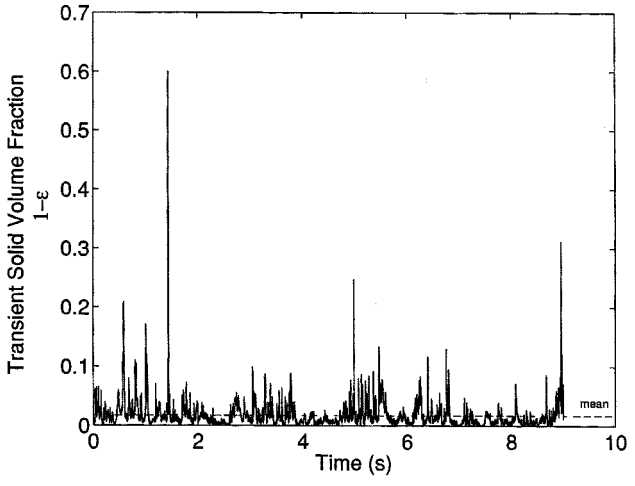

Figure 6. Typical output signal from the capacitance probe.

Comparison of the results from both techniques

As mentioned before, the solids concentration measurement by capacitance probes needs calibration. This might be done, for example, by reference to pressure gradients or to gamma-ray adsorption. A comparison of the absolute solids-concentration values obtained by both measurement techniques is therefore not meaningful, as the results are not independent of each other. However, an expressive comparison is possible for the shape of the concentration profiles, calculated as the relative deviation of the local solids concentration $\overline{\epsilon_s}(x,y)$ from the cross-sectional average $\langle\overline{\epsilon_s}\rangle$:

$$\frac{\overline{\epsilon_s}(x,y)-\langle\overline{\epsilon_s}\rangle}{\langle\overline{\epsilon_s}\rangle} = \text{solids fraction deviation from average.} \quad (2)$$

These nondimensional solids fraction profiles from capacitance probe readings and tomography are shown in Figure 7, for three different solid-mass fluxes, without a gas flow (v = 0 m/s). The orientation of the profiles is at the main vertical axis of the cross section related to the tomographic plots in Figure 5. A parabolic-shape distribution is observed, with deviations ranging from −75% up to+100% in relation to the

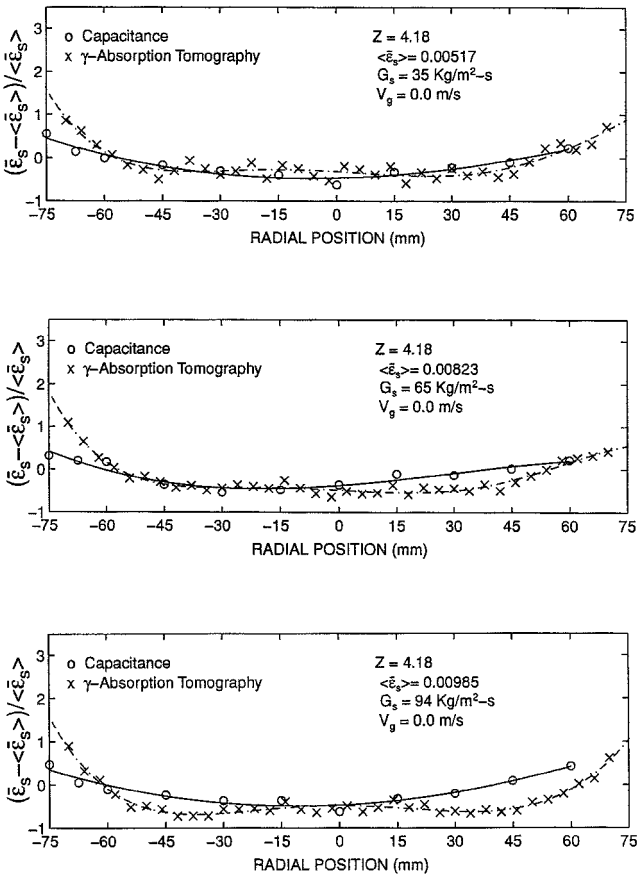

Figure 7. Comparison of radial solids concentration profiles from gamma tomography and capacitance probe readings: V_g = 0 m/s; different mass fluxes.

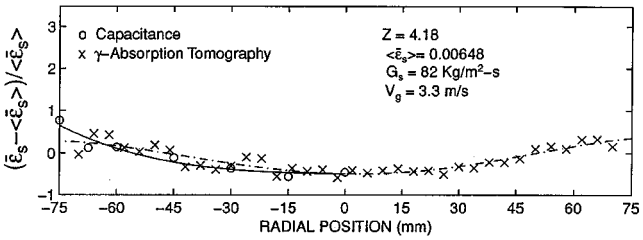

Figure 8. Comparison of radial solids concentration profiles from gamma tomography and capacitance probe readings: $V_g = 3.3$ m/s; $G_s \approx 82$ kg/(m^2·s).

cross-sectional average. The values from tomography at the closest radial position to the wall have been left out of these plots, because of the possible inaccuracy due to missing information in the projections at this position (see earlier). The agreement between gamma tomography and capacitance probe readings is very good, except in the vicinity of the wall. Here the readings from the capacitance probes show a smaller increase in solids fraction than do the values measured with tomography. We must remember that the tomography measurements are time-averaged solids fractions over 60−100 min, while the capacitance measurements are time-averaged solids fractions over ≈1 min. The good agreement between the two measured solids fractions, which are averaged over two different time intervals, reveals that local solids concentrations determined by the two measurement methods—capacitance sensing and γ-ray tomography—are both representative measurements for the downer flow. The shape of the profiles does not change significantly with increasing solids flux up to $\dot{m}_S = 94$ kg/(m^{2}s).

Figure 8 illustrates the concentration profiles for v = 3.3 m/s and $\dot{m}_S = 82$ kg/(m^{2}s). In this case, only half of the tube diameter was scanned with the capacitance probe. Again, there is good agreement between the two measurement techniques. In comparison to the solids flow without a gas flow (Figure 7), the solids fraction shows a more uniform shape, with deviations from the cross-sectional average ranging between $\pm 50\%$.

Increasing the superficial gas velocity to 6.6 m/s caused formation of solids strands in the downer, as was shown in Figure 5c. Figure 9 shows the solids concentration profile

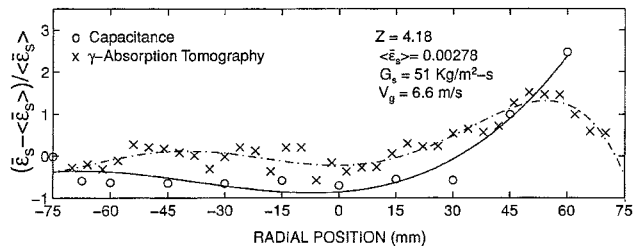

Figure 9. Comparison of radial solids concentration profiles from gamma tomography and capacitance probe readings: $V_g = 6.6$ m/s; $G_s \approx 51$ kg/(m^2·s).

from the horizontal main axis related to the tomographic plot in Figure 5c, thus crossing the solid strand in the right half of the cross section. In general, there is good agreement again between both measured profiles. The concentration peak seems to be emphasized more in the profile from the capacitance measurement.

Unfortunately there are no data collected from the radial positions close to the wall on the righthand side of the cross section because of the limited length of the probe. A possible explanation for the difference between the two measurements might be that the tomography smooths peaks in the profile due to the limited local resolution. Additionally, the tomography profile is a time average of more than 2 h of information, whereas each capacitance reading is averaged over only one minute.

Variation in the solids fraction along the length of the downer is shown in Figure 10. This figure contains measurements of local solids fractions for three elevations. These measurements were obtained by moving the capacitance probe to three elevations. The tomography setup was not movable, so there are tomography data for only one elevation. The data in the middle graph (elevation 2) again show good agreement between the solids fractions measured by the two methods. Again a solid strand is formed at a radial location between +30 and +65 mm. At this location, the capacitance probe readings indicate lower solids fractions than solids fractions gleaned from tomography readings. This is an indication of possible oscillations in local solids fraction over time. Cross-sectional solids fraction profiles from capacitance measurements are similar for the two upper elevations, indicating that the strand exists at the higher elevations. At the lowest elevation, however, the solids strand disappears and an almost uniform solids concentration profile is observed.

Conclusions

Local solids fraction measurements were obtained in a downer with gamma-absorption tomography as well as with capacitance probe techniques. Time-averaged local solids

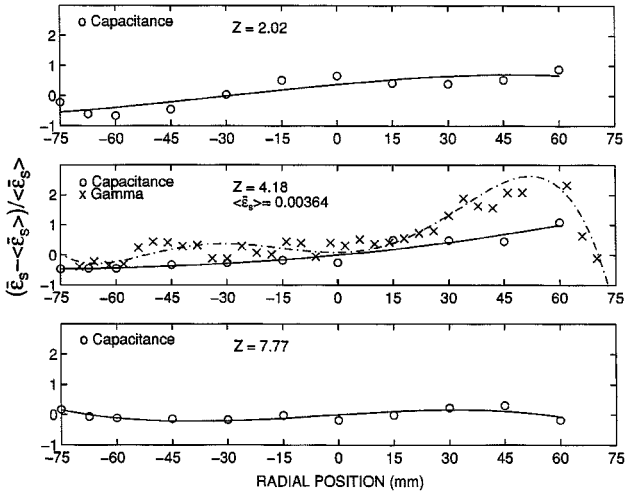

Figure 10. Variation of solids concentration profile with elevation: $V_g = 6.6$ m/s; $G_s = 71$ kg/(m^2·s).

fractions arrived at by both measurement techniques are compared for various operating conditions of the gas–solids flow. The following conclusions were derived:

- Tomography measurements require about 120-min recording time for an accurate measurement of local solids fractions.
- Although the capacitance probe can sense instantaneous variations in the local solids fraction, it must be integrated over at least a 1-min interval to get a representative measurement of time-averaged local solids fractions.
- In general, good agreement was observed between the solids concentration data using both measurement techniques. Capacitance probe measurements indicated lower solids concentration at radial locations close to the wall as compared to the solids fractions measured by tomography. Two possible causes are: tomography technique is less reliable in the line-averaged projection values at the edges of the tube, which is not recorded to reduce total measurement time; potential influence of the tube wall to capacitance probe measurements.
- Combined use of both measurement techniques offers the best chance to get time-averaged information about the concentration distribution over the whole cross section, as well as high-resolution information about the transient development of the flow at local positions of interest.

Acknowledgment

Financial support of the international cooperation and experimental investigations by the Alexander von Humboldt-Stiftung is gratefully acknowledged.

Notation

d_p = particle diameter, m
G_s = specific solids mass flow rate, kg $m^{-2} s^{-1}$)
L = length of the flow in the downer tube, m
ΔP = pressure difference caused by the solids, Pa
S = thickness of absorbing gas–solids flow, m
v = superficial gas velocity, $m \cdot s^{-1}$
x, y = radial coordinates, mm
z = elevation, mm
ρ_s = density of the solids, $kg \cdot m^{-3}$

Literature Cited

Galtier, P. A., R. J. Pontier, and T. E. Patureaux, "Near Full-Scale Cold Flow Model for the R2R Catalytic Cracking Process," *Fluidization VI*, Engineering Foundation, New York, p. 17 (1989).

Herb, B., K. Tuzla, and J. C. Chen, "Distribution of Solid Concentrations in Circulating Fluidized Bed," *Fluidization*, IV, Engineering Foundation, New York, p. 65 (1989).

Herb, B. E., "A Study of Solid Particle Distribution in Circulating Fluidized Beds," PhD Thesis, Lehigh Univ., Bethlehem, PA (1990).

Louge, M., "Experimental Techniques in Circulating Fluidized Beds," J. R. Grace, A. A. Avidan, and T. M. Knowlton, eds., Blackie, London, p. 312 (1997).

Schiewe, T., "Untersuchungen zum Einfluss der Gutaufgabevorrichtung auf die Strömungsmechanik in Fallrohrreaktoren," PhD Thesis, Univ. of Erlangen-Nürnberg, Erlangen, Germany (1997).

Seville, J. P. K., J. E. Morgan, and R. Cliff, "Tomographic Determination of the Voidage Structure of Gas Fluidized Beds in the Jet Region," *Fluidization V*, Engineering Foundation, New York, p. 87 (1986).

Soong, C. H., "An Experimental Investigation of Particle Clusters in Circulating Fluidized Bed," PhD Thesis, Lehigh Univ., Bethlehem, PA (1992).

Soong, C. H., K. Tuzla, and J. C. Chen, "Identification of Particle Clusters in Circulating Fluidized Beds," *Circulating Fluidized Bed Technology*, IV, Engineering Foundation, New York, p. 615 (1993).

Soong, C. H., K. Tuzla, and J. C. Chen, "Experimental Determination of Clusters Size and Velocity in Circulating Fluidized Beds," *Circulating Fluidized Bed Technology*, VIII, Engineering Foundation, New York, p. 219 (1995).

Wang, Z., F. Wei, Y. Jin, and Z. Yu, "Effect of Flow Direction on Hydrodynamics and Mixing of Circulating Fluidized Beds," Prepr. CFB V, Beijing, People's Republic of China (1996).

Zhu, J.-X, Z.-Q. Yu, Y. Jin, J. R. Grace, and A. Issangya, "Cocurrent Downflow Circulating Fluidized Bed (Downer) Reactors—A State of the Art Review," *Can. J. Chem. Eng.*, **73**, 662 (1995).

Manuscript received June 23, 1998, and revision received Feb. 5, 1999.